Acta Cryst. (1962). **15**, 786

A Study of Age-Hardening of Al-3·85% Cu by the Divergent X-ray beam Method

By T. Imura,* S. Weissmann and J. J. Slade, Jr.

College of Engineering, Rutgers — The State University, New Brunswick, N. J., U.S.A.

(*Received* 11 *January* 1961 *and in revised form* 18 *October* 1961)

Al-3·85% Cu single crystals were studied by means of the back-reflection divergent X-ray beam method after solution treatment, various modes of quenching and various stages of age-hardening. A complete strain analysis was developed by which the principal strains in a crystal or polycrystalline material can be determined provided the changes of d-spacings of more than six independent (hkl) reflections are recorded. The analysis applied to the various stages of age-hardening of crystals subjected to a fast quench after solution treatment disclosed an anisotropy of strain distribution in the matrix. The maximum strain corresponding to the ageing stage associated with the formation of G. P. zones coincided with one of the [100] directions and shifted about 20° when the θ' phase was predominant. The anisotropy of strain distribution was interpreted in terms of a preferred vacancy migration due to thermal and concentration gradients introduced by quenching.

1. Introduction

When an aluminum-rich aluminum–copper alloy is age-hardened, metastable transformation products are formed. These transformation products always precipitate on the {100} planes of the matrix and, consequently, these lattice planes may be regarded as the natural habit planes of the transformation products (Guinier, 1939, 1942; Preston, 1938).

The metastable transformation products, namely G.P. (II) and θ' phase, are coherent or partially coherent with the matrix and give rise to strains which, because of the difference in the size of the copper and aluminum atoms, assume considerable proportions.

It is the objective of this investigation to study systematically by means of a special high-resolution diffraction method the coherency strains set up between the matrix and the various transformation products. Beyond that an attempt is being made to elucidate through the analysis of the strain distribution the interconnection between vacancy migration and the nucleation sites of the transformation products.

2. Experimental procedure

A. *Specimen preparation*

The aluminum-3·85% copper single crystals were grown from the melt by the soft mold technique. Chemical analysis of the starting material showed that the content of Fe, Si, Mn, Mg, Zn, Zr, Ti and Ag was less than 0·00%. The single crystal platelets had a thickness of 1·5 mm. and were about 1×3 cm. in size. Prior to the solution heat treatment, they were carefully electropolished with Jacquet solution to remove the surface layers. The solution heat treatment was carried out at 540 °C. for 24 hr. to insure complete homogenization of the chemical composition. Subsequently most of the crystals were water-quenched, but some of them, by contrast, were also subjected to a quenching treatment in different media in order to study the effects of quenching on the strain distribution in the crystal. The crystals were then mounted on the X-ray unit and analyzed by the X-ray back-reflection divergent-beam method.

The controlled annealing necessary for the study of cold and warm hardening of the specimens was effected by means of an elliptical reflector lamp. This lamp was arranged in such a manner that the position of one of the focal points of the ellipsoid coincided with the filament of the incandescent bulb and that of the other focal point with the specimen surface. A thermocouple in contact with the specimen served to register the annealing temperature to better than ±1 °C. This heating arrangement proved to be very convenient and highly efficient.

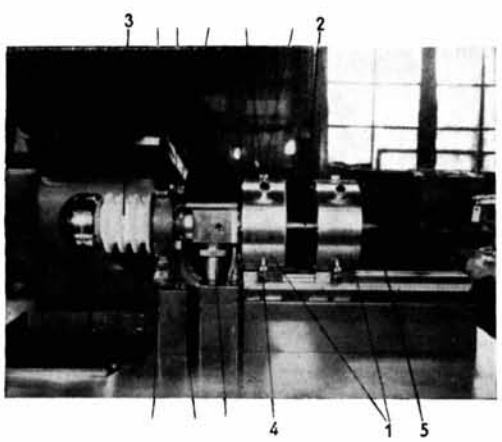

Fig. 1. Optical arrangement for capillary X-ray tube. 1) Electromagnetic lenses. 2) Capillary X-ray tube. 3) Electron gun. 4) Optical bench with precision scale to locate specimen and film position. 5) Tip of capillary tube.

* Present address: Institute for Solid State Physics, University of Tokyo, Azabu, Minato-Ku, Tokyo, Japan.

B. *Description of the back-reflection divergent-beam method*

This method is essentially a precision method for the determination of lattice parameters and anisotropic lattice distortions of single crystals. Although details of this method have been given elsewhere (Imura, 1954, 1957) a brief description pertinent to the latest development of apparatus and method will be offered here.

The divergent-beam method utilizes a horizontal capillary X-ray tube, shown in Fig. 1, in which an electron beam originating from an electron gun (3) is focused by means of electromagnetic lenses (1) onto the tip of a long capillary tube (5), where a thin metal foil is placed as an X-ray target. By operating the tube at a suitable voltage an X-ray beam with characteristic radiation emerges from the tip of the X-ray tube, exhibiting a divergence of nearly 180°. When this beam impinges on the test crystal, which is placed at a distance of 0–5 mm. from the tip of the capillary tube, diffraction patterns of the characteristic spectrum in transmission as well as in the back-reflection region are obtained as shown schematically in Fig. 2. To obtain good back-reflection patterns of aluminum and its alloys the distance of specimen to X-ray source employed varied between 3 and 4 mm. These patterns are analogous to the well known Kossel patterns except that in this case they are produced by an X-ray source located outside instead of inside the crystal. We have termed these patterns pseudo-Kossel patterns.

Of particular interest to the study of metal crystals are the back-reflection patterns (Figs. 4, 5, 7, 8). Referring to Fig. 2, it will be noted that each ellipse* of the pseudo-Kossel pattern corresponds to a reflection of a definite (*hkl*) set of planes. Consequently by indexing the reflections and by measuring x_1'' and x_2'', the coordinates of the extremities of the major axis of the ellipses, the lattice spacings of the individual (*hkl*) reflections and the lattice parameters can be determined with great precision. These measurements are carried out with the aid of the following relations (Imura, 1954):

$$\left.\begin{aligned} F'(x_1'') &= a\tan(\alpha-\beta)+2hb/(a+2b) \\ E'(x_2'') &= -a\tan(\alpha+\beta)-2hb/(a+2b) \\ \lambda &= 2d\sin\theta \end{aligned}\right\} \quad (1)$$

where the symbols have the following meanings:

α is the semi-apex angle of the incident X-ray cone equal to $\pi/2-\theta$, θ being the Bragg angle,
β is the angle subtended by the normal of the reflecting (*hkl*) plane and the axis of the capillary X-ray tube (perpendicular to the specimen surface),
a is the film distance from the X-ray source,
b is the specimen distance to the X-ray source,
$2h=\overline{E'F'}$ is the length of the major axis of the elliptical pattern,
d is the lattice spacing, and
λ the wavelength of the characteristic radiation concerned.

Since by this method the individual (*hkl*) reflections can be measured simultaneously, the anisotropic modifications in structure caused by an anisotropic strain distribution can be conveniently studied. Such anisotropic distortions of the lattice were observed during age-hardening and studied by this diffraction method.

It should be noted that in the present study a thin brass metal foil was used as X-ray target and consequently the pseudo-Kossel patterns obtained consisted of Cu $K\alpha$ as well as Zn $K\alpha$ lines (Figs. 4, 5, 7, 8). The use of the alloy target offered the additional advantage of carrying out precision lattice-parameter measurements as a function of wavelengths.

By determining the d-spacings of more than six independent (*hkl*) reflections and the corresponding changes which occur during the age-hardening process it was possible to carry out a complete strain analysis of the crystal and thus determine the principal strains for the various phases of age-hardening.

What follows is a theoretical treatment by which the principal strains have been determined.

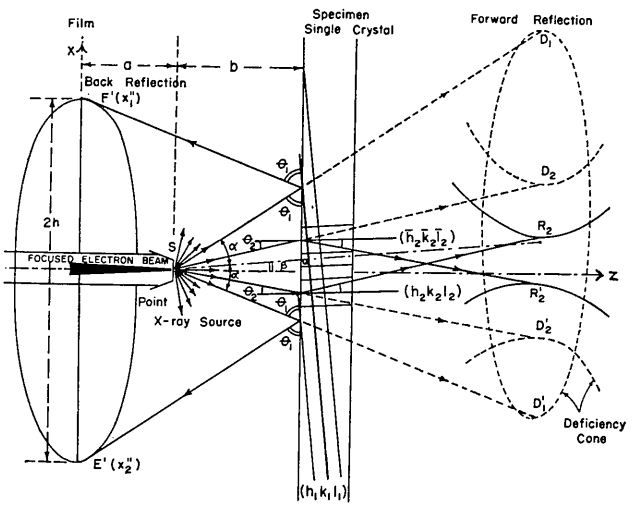

Fig. 2. Schematic representation of the generation of pseudo-Kossel patterns by the divergent beam method.

* Exactly speaking, the ellipse like figure on the film is a curve of higher orders. In this text, however, we call it 'ellipse' for brevity.

3. Analysis of strain

A. *General strain relations*

The state of strain of a solid is a point phenomenon which is completely described when the symmetric strain tensor T is given (Southwell, 1949). The diagonal elements of T are the normal strain components, and the sums of its symmetrically paired elements are the

shear components referred to a set of orthogonal axes through the point. The state of strain in a solid is usually inferred from measurements of finite displacements made on solid boundaries.

The X-ray divergent beam method described above yields information about the state of strain of a crystal in a finite but small neighborhood of a point, not by indicating the displacements of the boundary of the neighborhood, but by yielding pseudo-Kossel curves deformed by the changes in Bragg angles that occur around the reflecting ellipses on the crystal surface. On this account it will be necessary to employ a statistical algorithm to infer an average state of strain from measurements of the elements of the recorded curves.

In the following discussion a simplified matrix notation will be used in which vectors are column matrices (Patterson, 1959). Here vectors will be represented by ordinary letters such as x and H, which will be identified as such in the text. If x is a column matrix, the transposed row matrix $x' = (x_1, x_2, \ldots, x_n)$ will represent the same n-vector.

The nine components of the strain tensor are

$$\varepsilon_{ii} = (\partial u_i/\partial x_i);\ \tfrac{1}{2}\varepsilon_{ij} = \tfrac{1}{2}((\partial u_j/\partial x_i) + (\partial u_i/\partial x_j)), \quad i, j = 1, 2, 3, \tag{2}$$

where u is a vector point function that represents the deformation of the solid. If n is a unit vector, the normal strain component in the direction of n is

$$s_n = n'Tn, \tag{3}$$

and if m is a unit vector perpendicular to n the shear component associated with m, n is

$$s_{mn} = 2m'Tn. \tag{4}$$

The principal strains are the eigenvalues $\lambda = \lambda_1, \lambda_2, \lambda_3$, of the homogeneous system

$$Tn = \lambda n. \tag{5}$$

These are the roots, known to be real, of the cubic

$$\mathrm{Det}\,(T - \lambda I) = 0, \tag{6}$$

in which I is the unit matrix. The principal axes coincide with the eigenvectors $n = n_1, n_2, n_3$, obtained by solving the homogeneous system

$$(T - \lambda_r I)n = 0;\ r = 1, 2, 3. \tag{7}$$

In this reference system T is reduced to a diagonal matrix.

B. *The average strain tensor*

X-ray diffraction techniques may be used to yield information about the state of strain of a crystal in the neighborhood of a point by exhibiting measurable shifts in the location of the diffraction maxima. These maxima result through an averaging process over the irradiated volume of the crystal. In particular, the X-ray divergent beam method described above yields pseudo-Kossel patterns deformed by the small changes in Bragg angle that occur around the reflecting ellipses on the surface of the crystal. On this account it will be necessary to employ a statistical algorithm to infer an average state of strain from the recorded lattice spacing changes.

For reference we take a point within the irradiated volume of the crystal with three mutually perpendicular axes through it. The unit vectors on these lines will be designated by i, j, k. When the crystal is cubic these will coincide with the crystallographic direction (100), (010), (001); then the components of the vector $H = (hkl)$ are direction numbers for the family of planes H. In the non-cubic crystal it will be necessary to transform the Miller indices (hkl) to $(H_iH_jH_k)$, the components of the normal to the planes H in the directions ijk. Although the Al–Cu system considered here is cubic the explicit relations for $(H_iH_jH_k)$ are presented for completeness.

The basic tetrahedron of the crystal lattice may be referred to an ijk system as in Fig. 3. Then the direction numbers $(H_iH_jH_k)$ of the normal to the (hkl) plane (that is, the plane that passes through the points $a/h(100)$, $b/k(010)$, $c/l(001)$ are given by the determinants

$$H_i = hkl/(bc)\begin{vmatrix} 0 & 0 & 1 \\ (b/k)\sin\gamma & 0 & 1 \\ (c/l)\cos\beta\sin\alpha & (c/l)\sin\beta & 1 \end{vmatrix},$$

$$H_j = -hkl/(bc)\begin{vmatrix} a/h & 0 & 1 \\ (b/k)\cos\gamma & 0 & 1 \\ (c/l)\cos\beta\cos\alpha & (c/l)\sin\beta & 1 \end{vmatrix},$$

$$H_k = hkl/(bc)\begin{vmatrix} a/h & 0 & 1 \\ (b/k)\cos\gamma & (b/h)\sin\gamma & 1 \\ (c/l)\cos\beta\cos\alpha & (c/l)\cos\beta\sin\alpha & 1 \end{vmatrix}. \tag{8}$$

The factor hkl/bc reduces H_i, H_j, H_k to dimensionless linear function of h, k, l.

In what follows the crystal is assumed to be cubic; if the crystal is not cubic then H_i, H_j, H_k are substituted for h, k, l wherever these occur in the following discussion.

Equations (3) and (4) may now be written

$$|H|^2 s_n = H'TH,$$
$$|H_1||H_2|s_{12} = 2H_1'TH_2. \tag{9}$$

It will generally not be possible to observe the small relative shifts in reflexion maxima that result from shearing strains, so that only the first of these equations may be used to determine the state of strain. The strain components may be measured and computed as fractional change ($\Delta d/d$) or *per cent* change ($100\,\Delta d/d$) in lattice spacing. In either case they will be referred to as strains or as relative change in spacing.

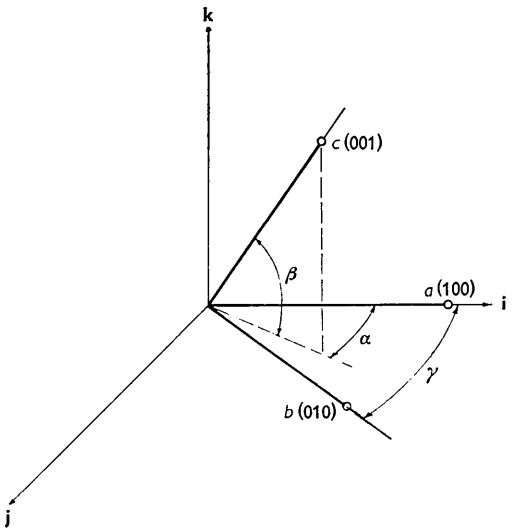

Fig. 3. Relation of (hkl) to $(H_iH_jH_k)$ in non-cubic crystals.

Let $s_n = s_r$ be the relative change in spacing of the H_r-planes. The first of equations (9), which is a quadratic form, may be written

$$|H_r|^2 s_r = \alpha_r' \eta \,, \tag{10}$$

in which α_r and η are the 6-vectors

$$\begin{aligned} \alpha_r' &= (h_r^2, k_r^2, l_r^2, k_r l_r, l_r h_r, h_r k_r) \,, \\ \eta' &= (\varepsilon_{11}, \varepsilon_{22}, \varepsilon_{33}, \varepsilon_{23}, \varepsilon_{31}, \varepsilon_{12}) \,. \end{aligned} \tag{11}$$

In order to determine the six components of η or, equivalently, the nine components of T as shown by equations (2), it will be necessary to measure the lattice spacing in six crystallographic directions H_r, $r = 1, 2, \ldots, 6$. Each measurement leads to an equation of type (10) and the set of six may be written

$$\beta = A\eta \,, \tag{12}$$

in which β is a 6-vector with components $|H_r|^2 s_r$, and A is a 6×6 matrix with the components of α_r' as the elements of its rth row.

This matrix equation may be solved for η provided that $\mathrm{Det}\, A \neq 0$; that is, provided that the six sets of numbers (h_r, k_r, l_r) lead to a matrix of rank six. Generally there appears to be no simple way to decide whether a particular set H_r, $r = 1, 2, \ldots, 6$ is suitable without constructing A and testing it in the usual way. If the set of vectors H_r consists of two subsets of three mutually orthogonal vectors, then $\mathrm{Det}\, A = 0$. This is true because the linear invariant of the cubic (6) is the sum of the diagonal elements of T, $I_1 = \varepsilon_{11} + \varepsilon_{22} + \varepsilon_{33}$, and this relation reduces the six readings to five independent readings.

For example, readings taken in the six directions (200), (020), (002), (333), $(2\bar{4}2)$, $(20\bar{2})$ are not sufficient because the first three and the last three vectors are orthogonal subsets. On the other hand the determinant associated with the vectors (200), (020), (002), (111), $(11\bar{1})$, $(1\bar{1}1)$ is not zero and the set is acceptable.

As an illustration of the difficulties that may result in attempting to find the state of stress we take the set of relative spacing changes obtained by the divergent beam method which are presented in Table 1.

Table 1. *Relative spacing changes*

r	h_r	k_r	l_r	s_r
1	2	2	4	0·45
2	0	2	4	0·44
3	$\bar{1}$	1	5	0·35
4	1	1	5	0·29
5	3	3	3	0·15
6	2	4	2	0·20

For this set the explicit form of the matrix equation (12) becomes

$$\begin{bmatrix} 24\times 0{\cdot}45 \\ 20\times 0{\cdot}44 \\ 27\times 0{\cdot}35 \\ 27\times 0{\cdot}29 \\ 27\times 0{\cdot}15 \\ 27\times 0{\cdot}20 \end{bmatrix} = \begin{bmatrix} 4 & 4 & 16 & 8 & 8 & 4 \\ 0 & 4 & 16 & 8 & 0 & 0 \\ 1 & 1 & 25 & 5 & -5 & -1 \\ 1 & 1 & 25 & 5 & 5 & 1 \\ 9 & 9 & 9 & 9 & 9 & 9 \\ 4 & 16 & 4 & 8 & 4 & 8 \end{bmatrix} \begin{bmatrix} \varepsilon_{11} \\ \varepsilon_{22} \\ \varepsilon_{33} \\ \varepsilon_{23} \\ \varepsilon_{31} \\ \varepsilon_{12} \end{bmatrix} .$$

It may be verified that the rank of this matrix is 5, so that the six sets of planes shown in Table 1 are not independent. By successive elimination it is found that $\varepsilon_{31} + \varepsilon_{12} = 0{\cdot}45$, also that $\varepsilon_{31} + \varepsilon_{12} = 2{\cdot}65$, which shows that the readings are not consistent.

Such inconsistencies are to be expected. The divergent beam method yields a vector β with components that are faulty estimates of a set of normal strains near some point within the crystal. For example, there are errors inherent in the measurement of the diameters of the pseudo-Kossel figures. Also, the evidence of change in lattice spacing is obtained as the result of diffraction over a conic section which traverses a sequence of states of strain. Two pseudo-Kossel figures come from different parts of the crystal, so that it is quite possible, for instance, to obtain different relative strains from measurements of the figures resulting simultaneously from the (111) and (333) reflections.

If A is of rank 6 the inconsistency in the measurements does not appear, since a unique set of strains is computed. But the computed strain system would almost surely be in error, without there being an indication of the magnitudes of the errors. To minimize these errors it will be necessary to record more than six strains and to use the method of least squares to determine an average value of η, and thus of T, within the irradiated region. The redundancy in measurement seems also to be required as the simplest way to ensure an independent set of directions, for if any selection of six out of $N > 6$ yields a matrix of rank 6, the possibility of computing the components of T is assured. The redundancy does not, of course, ensure this; it merely enhances the chance of success.

When the number N of readings is greater than 6 then, instead of the matrix equation (12), one may construct the normal matrix equation

$$\beta^* = A^* \langle \eta \rangle \tag{13}$$

from which to determine the average vector $\langle \eta \rangle$, and thence the average tensor $\langle T \rangle$. Using the notation

$$[abc\ldots] = \sum_{r=1}^{N} a_r b_r c_r \ldots$$

equation (13) may be written

$$\begin{bmatrix} [h^2|H|^2 s] \\ [k^2|H|^2 s] \\ [l^2|H|^2 s] \\ [kl|H|^2 s] \\ [lh|H|^2 s] \\ [hk|H|^2 s] \end{bmatrix} = \begin{bmatrix} [h^4] & [h^2k^2] & [h^2l^2] & [h^2kl] & [h^3l] & [h^3k] \\ [h^2k^2] & [k^4] & [k^2l^2] & [k^3l] & [hk^2l] & [hk^3] \\ [h^2l^2] & [k^2l^2] & [l^4] & [kl^3] & [hl^3] & [hkl^2] \\ [h^2kl] & [k^3l] & [kl^3] & [k^2l^2] & [hkl^2] & [hk^2l] \\ [h^3l] & [hk^2l] & [hl^3] & [hkl^2] & [h^2l^2] & [h^2kl] \\ [h^3k] & [hk^3] & [hkl^2] & [hk^2l] & [h^2kl] & [h^2k^2] \end{bmatrix} \begin{bmatrix} \langle \varepsilon_{11} \rangle \\ \langle \varepsilon_{22} \rangle \\ \langle \varepsilon_{33} \rangle \\ \langle \varepsilon_{23} \rangle \\ \langle \varepsilon_{31} \rangle \\ \langle \varepsilon_{12} \rangle \end{bmatrix}.$$

With these values of $\langle \varepsilon_{ij} \rangle$, the average strain components in the i, j, k system, the cubic (6) may be constructed and its roots determined. These three roots will be the principal average strains, the directions corresponding to them in the mean being found by solving the three homogenous systems (7).

This analysis, of course, is not affected by the particular technique that may be used to determine the changes in lattice spacing. It is applicable to the study of polycrystalline materials as well as to that of single crystals so long as d-spacing changes result in strains.

C. *Computation*

The facilities of an I.B.M. 650 were used for the computation of the $\langle \varepsilon_{ij} \rangle$ and for the determination of the principal strains and principal axes.

Using a routine programmed under the title 'Matrix Inversion by Gaussian Elimination' (Gardner, 1956), equation (13) was solved for the general case when β^* is a $6 \times b$ matrix, with b representing the number of different sets of readings of the strains s, all referred to the same (h, k, l) planes.

The principal strains and axes were determined using the program headed 'Latent Roots and Vectors of a Matrix' (Granet, 1958), which give the latent roots, or principal strains, in order of magnitude, and their corresponding vectors, or principal axes. The latter are scaled so that the largest component of a vector is normalized to unity.

Table 2 shows the results of three sets of strain components, each consisting of eight determinations

Table 2. *Strain components corresponding to different heat treatments of* Al-3·85% Cu *crystal*

A $(\Delta d/d)100$	B $(\Delta d/d)100$	C $(\Delta d/d)100$	h	k	l
−0·06	0·24	0·30	0	2	4
0·02	0·17	0·21	2	2	4
−0·02	0·13	0·20	1	3	3
0·13	0·11	0·11	3	3	3
0·08	0·13	0·16	$\bar{1}$	1	5
0·00	0·19	0·17	$\bar{1}$	$\bar{1}$	5
0·00	0·15	0·15	1	1	5
0·13	0·19	0·16	3	3	3

A annealed at 205 °C. for 20 hr. Mixture of G.P. [II] and some θ'.
B annealed as in *A* plus 320 °C. for ½ hr. Predominantly θ'.
C annealed as in *A* + *B* + 430 °C. for 23 hr. θ phase.

of relative changes in d-spacing as measured by the divergent beam method. These three sets correspond to different heat treatments of the specimen and, therefore, to the presence of different phases or mixture of phases in the age hardening process.

The presence of these transformation phases was checked by X-ray and hardness tests and agreed with the findings of Silcock *et al.* (Silcock, Heal & Hardy, 1953–54, 1955–56).

Three sets of eight equations of the form (12) are obtained in the same way as illustrated by example of Table 1. From these, equation (13), with $b = 3$ becomes:

$$\begin{bmatrix} 182 & 190 & 310 & 208 & 30 & 20 \\ 190 & 278 & 446 & 312 & 54 & 44 \\ 310 & 446 & 2630 & 672 & 30 & 116 \\ 208 & 312 & 672 & 446 & 116 & 54 \\ 30 & 54 & 30 & 116 & 310 & 46 \\ 20 & 44 & 116 & 54 & 46 & 19 \end{bmatrix} \begin{bmatrix} \langle \varepsilon_{11} \rangle \\ \langle \varepsilon_{22} \rangle \\ \langle \varepsilon_{33} \rangle \\ \langle \varepsilon_{23} \rangle \\ \langle \varepsilon_{31} \rangle \\ \langle \varepsilon_{12} \rangle \end{bmatrix} = \begin{bmatrix} 101{\cdot}99 & 95{\cdot}05 & 33{\cdot}12 \\ 155{\cdot}99 & 137{\cdot}61 & 24{\cdot}88 \\ 585{\cdot}35 & 537{\cdot}21 & 10{\cdot}48 \\ 203{\cdot}53 & 167{\cdot}67 & 20{\cdot}84 \\ 42{\cdot}27 & 15{\cdot}99 & -22{\cdot}36 \\ 48{\cdot}57 & 38{\cdot}97 & -25{\cdot}04 \end{bmatrix} \tag{14}$$

Using the matrix inversion technique indicated above it can be verified that the rank of A^* is six.

Three sets of $\langle \varepsilon_{ij} \rangle$'s are thus obtained which, when substituted in equation (6), will give three sets of latent roots and their associated vectors.

For instance, using the third column of (14) the following values are obtained

$$\begin{aligned} \langle \varepsilon_{11} \rangle &= \ \ 0{\cdot}2791 \\ \langle \varepsilon_{22} \rangle &= -0{\cdot}0644 \\ \langle \varepsilon_{33} \rangle &= -0{\cdot}0175 \\ \langle \varepsilon_{23} \rangle &= \ \ 0{\cdot}0228 \\ \langle \varepsilon_{31} \rangle &= -0{\cdot}0764 \\ \langle \varepsilon_{12} \rangle &= -0{\cdot}1236\,. \end{aligned} \tag{15}$$

Equation (6) becomes

Table 3. *Principal strains in age-hardened* Al–3·85% Cu *crystal, water-quenched after solution treatment*

Heat treatment	Phases present	Maximum strain λ_1				Intermediate strain λ_2				Minimum strain λ_3			
		Magnitude in %	Direction number		Direction	Magnitude in %	Direction number		Direction	Magnitude in %	Direction number		Direction
205 °C. for 20 hr.	G.P. [II] + some θ'	0·41	n_1	0·05	u 0	0·18	n_1	0·17	u 0	−0·10	n_1	1·00	u 1
			n_2	1·00	v 1		n_2	0·17	v 0		n_2	−0·08	v 0
			n_3	−0·18	w 0		n_3	1·00	w 1		n_3	−0·15	w 0
Additional annealing at 320 °C. for ½ hr.	θ'	0·47	n_1	0·04	u 0	0·15	n_1	0·15	u 0	−0·03	n_1	1·00	u 1
			n_2	1·00	v 3		n_2	0·37	v 1		n_2	−0·08	v 0
			n_3	−0·37	w $\bar{1}$		n_3	1·00	w 3		n_3	0·12	w 0
Additional annealing at 430 °C. for 23 hr.	Matrix + incoherent θ (equilibrium phase)	0·29	n_1	1·00	u 1	−0·08	n_1	0·16	u 0	−0·02	n_1	0·14	u 0
			n_2	−0·18	v 0		n_2	1·00	v 1		n_2	0·06	v 0
			n_3	−0·13	w 0		n_3	−0·09	w 0		n_3	1·00	w 1

$$\begin{vmatrix} 0{\cdot}2791-\lambda & -0{\cdot}0618 & -0{\cdot}0382 \\ -0{\cdot}0618 & -0{\cdot}0644-\lambda & 0{\cdot}0114 \\ -0{\cdot}0382 & -0{\cdot}0114 & -0{\cdot}0175-\lambda \end{vmatrix} = 0 . \quad (16)$$

Using the computation routine indicated above, the following latent roots are obtained

$$\begin{aligned} \lambda_1 &= \ \ 0{\cdot}29 \\ \lambda_2 &= -0{\cdot}08 \\ \lambda_3 &= -0{\cdot}02 . \end{aligned} \quad (17)$$

Substituting each of these roots in equation (7), three sets of homogenous equations are obtained for the solution of the vectors, or principal axes, associated with the corresponding eigenvalues. For instance, for $\lambda_1 = 0{\cdot}290$, one obtains from equation (7):

$$\begin{pmatrix} -0{\cdot}0109 & -0{\cdot}0618 & -0{\cdot}0382 \\ -0{\cdot}0618 & -0{\cdot}3544 & 0{\cdot}0114 \\ -0{\cdot}0382 & 0{\cdot}0114 & -0{\cdot}3075 \end{pmatrix} \begin{pmatrix} n_1 \\ n_2 \\ n_3 \end{pmatrix} = 0 . \quad (18)$$

The values of n_1, n_2 and n_3, with the largest value normalized to one are:

$$\begin{aligned} n_1 &= \ \ 1{\cdot}00 \\ n_2 &= -0{\cdot}18 \\ n_3 &= -0{\cdot}13 . \end{aligned} \quad (19)$$

The complete solution for the three sets shown in Table 2 are given in Table 3.

4. Experimental results

A great number of pseudo-Kossel patterns of the Al-3·85% Cu crystals were taken as a function of ageing, but only the most representative and relevant ones to the strain analysis will be shown here. Fig. 4 exhibits the pseudo-Kossel pattern obtained immediately after water quenching from the solution heat treatment at 540 °C.

Comparison of the d-values obtained after quenching with those obtained at the solution heat treatment temperature showed that the thermal stresses resulting from quenching had virtually no effect on the d-values. If, upon quenching, any variations in the d-values occurred, they were at least by orders of magnitude smaller than the effect introduced by the strains associated with the formation of aggregates or precipitates of solute atoms. Consequently the d-values of the quenched specimen could be safely used as reference in the determination of the strain values $\Delta d/d$ of the aged specimens listed in Table 2.

Two salient features characterized the patterns of the aged specimens. One was line broadening and the other was line shift with respect to the reference pattern. The broadening effect is undoubtedly associated with the lattice distortions incurred by the matrix and is due to the coherency strains set up between the metastable transformation products and the matrix. The line shift $\Delta d/d$ is associated with lattice expansion or contraction and results principally from two effects. One is due to the coherency strains described above and the other due to the volume expansion of the matrix resulting from the precipitation of the smaller copper atoms into zones, leaving behind a matrix rich in larger aluminum atoms.

Fig. 5 represents the pattern obtained for the specimen aged at 205 °C. for 20 hours (ageing treatment A) and corresponds principally to a mixture of G.P. [II] with some admixture of θ'. An anisotropy of line broadening was observed, since for the (333), ($\bar{3}33$), (115) and ($\bar{1}15$) reflections this effect was particularly pronounced. The line broadening effect was in the direction of lattice expansion and the sequence of Fig. 6 which represents a photometric tracing of the (333) line profile as a function of ageing affords a graphic visualization of this broadening effect. It is interesting to note that the intensity distribution of the $K\alpha_1$ and $K\alpha_2$ profile exhibited multiple peaks (Fig. 6) which is indicative of a complex substructure of the matrix resulting from the coherency strains.

The line shift $\Delta d/d$ for this aged specimen was also anisotropic and for the observable reflection attained its largest value for the (333) reflection (Table 2).

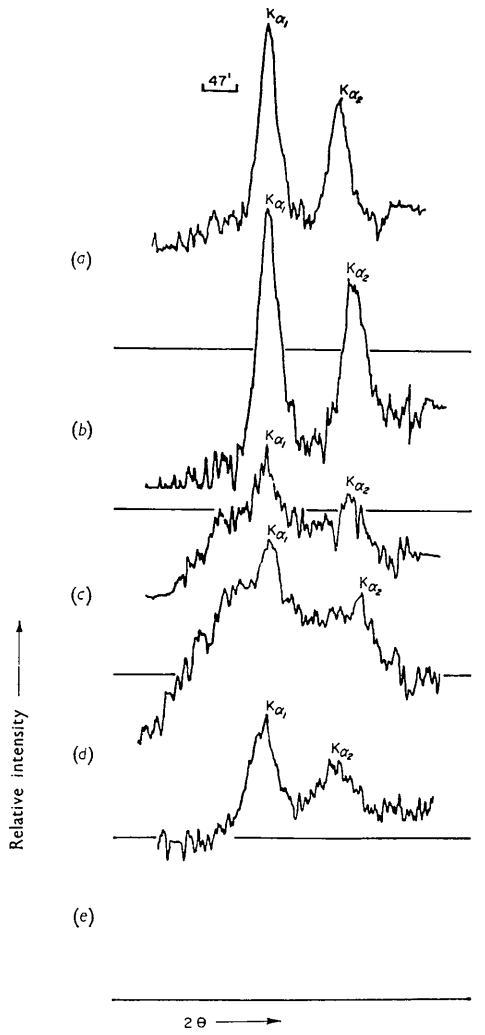

Fig. 6. Effect of ageing on the line profile of (333) matrix reflection. Recording microphotometer tracing. (*a*) As quenched from 540 °C. (*b*) Aged at 100 °C. for 96 hr. (principally G.P. [I] zones present). (*c*) Aged at 205 °C. for 20 hr. (G.P. [II] + some θ'). (*d*) Aged at 205 °C. for 50 hr. (G.P. [II] + θ'). (*e*) Aged at 320 °C. for one-half hr. (θ').

After continued ageing at 320 °C. for one half hour (ageing treatment *B*) the G.P. zones had disappeared and only the θ' phase was prevalent. In contradistinction to the line broadening produced by the treatment *A* the line broadening resulting from treatment *B* affected all (*hkl*) lines. Furthermore, the broadening was not solely in the direction of lattice expansion but was nearly uniform in all directions with respect to the position of the peak intensity. This resulted in a sharp decrease in the resolution of the $K\alpha$ doublets (Figs. 5 and 6). The line shift, however, was anisotropic, occurring in the direction of lattice expansion, and as shown in column 2 of Table 2 was most salient for the (024) reflection.

Fig. 7 represents a composite diagram of the pseudo-Kossel pattern pertaining to the ageing treatment *B* superimposed over that obtained after solution heat treatment and subsequent water quenching. This composite diagram may serve to aid the visual realization of the anisotropic matrix expansion.

Annealing at 430 °C. for 23 hr. followed by slow cooling (ageing treatment *C*) established the equilibrium phase θ and therefore eliminated the coherency strains associated with the preceding metastable transformation products. Consequently, in Fig. 8 the lines became sharp and the resolution of the $K\alpha$ doublet was again restored.

5. Discussion

As may be seen from Table 3 the principal strains associated with ageing treatment *A* have such directions that the (010) cube planes may be identified as the principal habit planes on which the G.P. zones have formed. It appeared, however, that the formation of the G. P. zones did not take place uniformly on all {100} planes but favored a certain set of planes, namely (010). This became apparent from the direction of the principal strain, λ_1, which is associated with the matrix distortion of the (010) planes. Precipitation of the G.P. zones must have occurred to a lesser degree on the (001) planes and was practically negligible on the (100) planes, since for these planes the magnitude of the minimum strain, λ_3, assumes an appreciable negative value, namely $-0{\cdot}10\%$.

The largest value for the maximum strain in the matrix was reached when the partially coherent θ' precipitate was formed (ageing treatment *B*) and it is interesting to note that the maximum hardness obtained during ageing corresponds precisely to this stage of matrix deformation (Silcock, Heal & Hardy, 1955–56; Hardy & Heal, 1956). It is also worth noting that the maximum strain no longer is perpendicular to the (010) planes but more nearly perpendicular to the $(03\bar{1})$ planes. This implies that, due to the preponderance of θ', the direction of the maximum strain has shifted about 20° from that exerted predominantly by the G.P. zones. Such a shift in the direction of the principal strain would be expected if we take into account the fact that the θ' platelets precipitate preferentially on dislocation helices. The latter are said to be formed by the winding up of screw dislocation about their axes as a result of the condensation of excess vacancies retained by quenching (Thomas & Whelan, 1959; Thomas & Nutting, 1959). The precipitation of G.P. zones, on the other hand, is not associated with the dislocation helices and their nucleation sites appear to be unaffected by the existing dislocation network of the matrix (Nutting).

Finally, it should be pointed out that the strain analysis of the matrix disclosed still a strain distribution for the ageing treatment *C* which resulted in the precipitation of the incoherent θ equilibrium phase. From this one may conclude that the interface formed

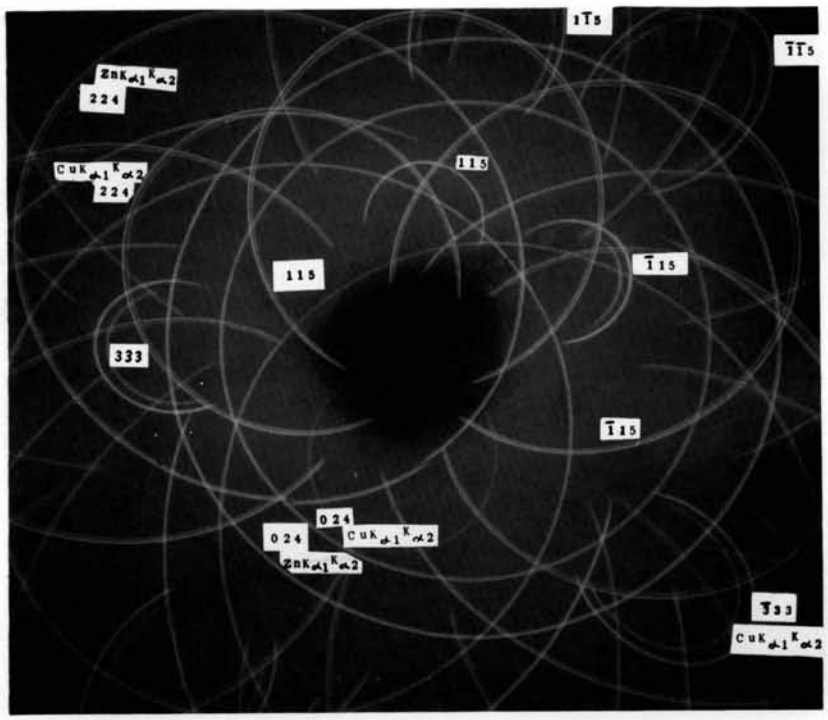

Fig. 4. Back-reflection divergent beam pattern of Al-3·85% Cu.
Solution heat-treated at 540 °C. and water-quenched.

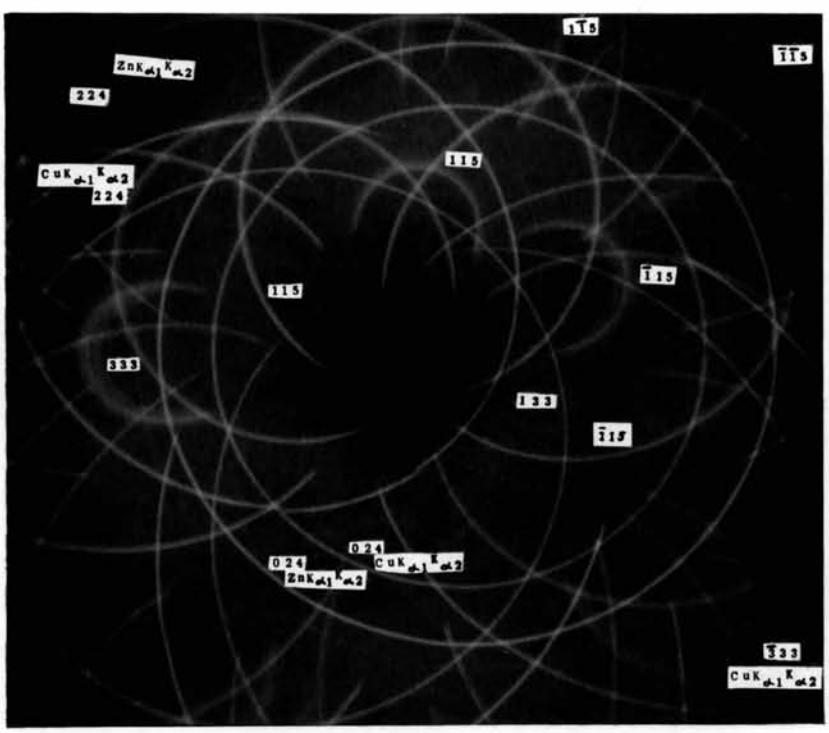

Fig. 5. Back-reflection divergent beam pattern of Al-3·85% Cu.
Aged for 20 hr. at 205 °C. after the heat treatment mentioned in the legend of Fig. 4.

[*To face p.* 792

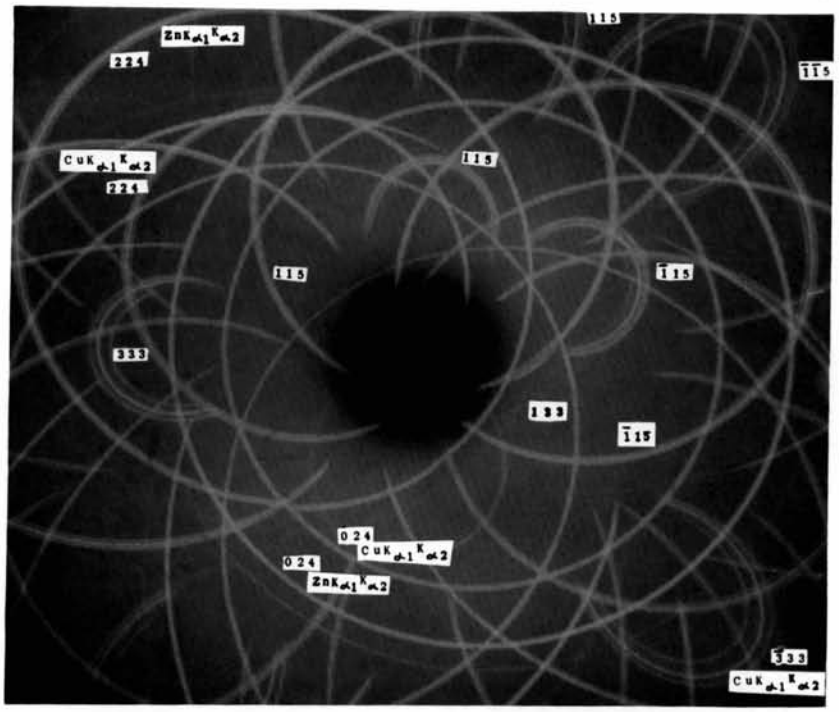

Fig. 7. Back-reflection divergent beam pattern of Al-3·85% Cu.
Superposition of two patterns, one for the specimen quenched from 540 °C. and the other for the same specimen followed by ageing for one-half hr. at 320 °C., exhibiting anisotropic lattice expansion.

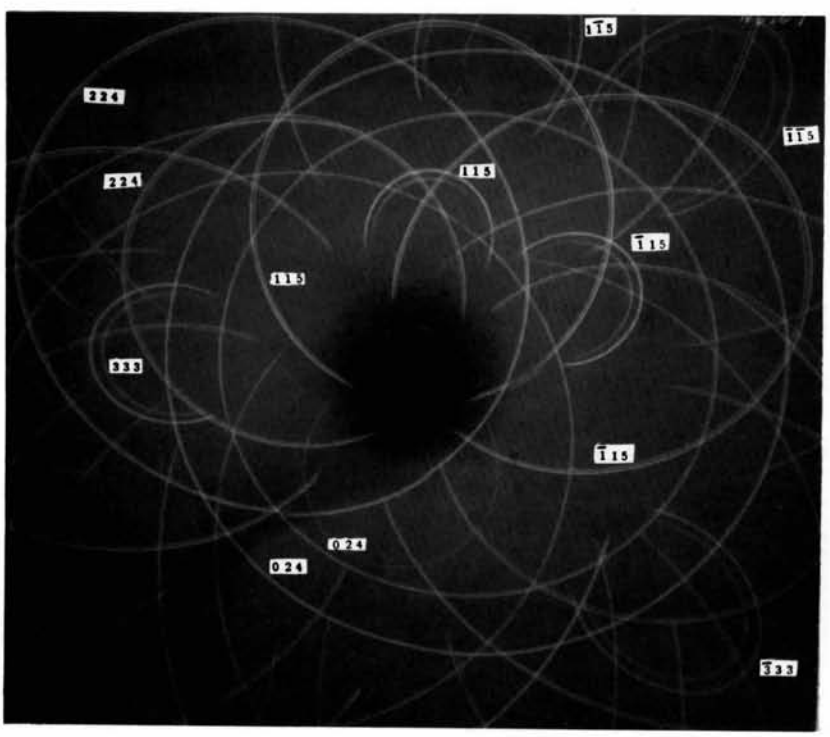

Fig. 8. Back-reflection divergent beam pattern of Al-3·85% Cu.
Aged at 430 °C. for 23 hr. Note the return of sharpness of the matrix reflections after precipitation of θ phase.

between the partially coherent θ' precipitate and the matrix consisted of a dislocation network which upon continued ageing could not be entirely removed.

When ageing experiments were performed after quenching in less drastic media than water, namely mineral oil (slow quench), it was disclosed by the divergent beam method that nearly isotropic lattice deformation of the matrix was obtained. It appeared, therefore, that the anisotropy of lattice distortions, besides being dependent on the shape of the specimen, was intimately linked with the mode of quenching. In the light of these experimental observations one may explain the resulting anisotropy principally by two interdependent effects, both of which would cause a preferred directional migration of quenched-in excess vacancies and thus lead to a directional biasing for the nucleation sites of the G.P. zones. These two effects introduced by quenching are: 1) thermal gradient, and 2) concentration gradient of quenched-in excess vacancies.

The effect of these gradients on the formation of preferred nucleation may be visualized as follows: Immediately upon quenching the specimen surface reaches a temperature value which is considerably lower than that of the interior. Since the thickness of the specimen platelet is small compared to the other size dimensions the migration of vacancies will no longer follow a random walk but will be principally controlled by the thermal gradient and consequently will predominantly occur in the direction parallel to the specimen thickness. This implies that a concomitant diffusion of the copper atoms would take place in the same preferred direction but in the opposite sense from that of the vacancy migration. In addition one has to take into consideration that at the specimen surface the concentration of the quench-in vacancies in excess of the equilibrium concentration is greater than in the interior and that under the influence of the thermal gradient a migration of these excess vacancies will also take place parallel to the specimen thickness. Thus the preferred diffusion direction of the copper atoms would lead to preferred nucleation sites of the G.P. zones and to concomitant anisotropic lattice distortion of the matrix. As expected, the preferred nucleation sites will depend on the specimen orientation, that is, on the orientation of the (001) planes relative to the preferred diffusion direction. They will reach a maximum value for (001) planes perpendicular and a minimum value for those parallel to the preferred diffusion direction.

In support of the concept of preferential vacancy migration from the surface to the interior it should be pointed out that recent microscopic examinations of metals injected with helium by using them as targets of energetic alpha particles revealed the free surfaces as the principal suppliers of vacancies (Barnes, 1960).

In conclusion it should be noted that the biasing of nucleation sites of the G.P. zones may have an important practical implication, since it may be possible to effect directional hardening of alloys by a suitable selection of specimen shape and quenching medium.

The authors wish to express their thanks for the valuable assistance which Prof. L. Nanni gave to the computer programming of the strain analysis, and to Mr Y. Nakayama for his help in the experimental work. The support of this work by the Office of Naval Research under Contract NONR 404 (09) is gratefully acknowledged.

References

BARNES, R. S. (1960). *Phil. Mag.* **5**, 635.
GARDNER, A. O. (1956). *Matrix Inversion by Gaussian Elimination*. I. B. M. Houston; File Number 5.2.002.
GRANET, W. (1958). *Latent Roots and Vectors of a Matrix*. Boston, Mass.: Boston University; File Number 5.2.016.
GUINIER, A. (1939). *Ann. Phys.* XI, **12**, 161.
GUINIER, A. (1942). *J. Phys. Radium* VIII, **3**, 129.
HARDY, H. K. & HEAL, T. J. (1956). *The Mechanism of Phase Transformation in Metals*, p. 1. London: Institute of Metals.
IMURA, T. (1954). *Bull. Naniwa Univ.* A, **2**, 51.
IMURA, T. (1957). *Bull. Univ. Osaka Pref.* A, **5**, 99.
NUTTING, J. (private communication).
PATTERSON, A. L. (1959). *International Tables for X-ray Crystallography*, p. 11. Birmingham: Kynoch Press.
PRESTON, G. D. (1938). *Proc. Royal Soc.* A, **167**, 526.
SILCOCK, J. M., HEAL, T. J. & HARDY, H. K. (1953–54). *J. Inst. Met.* **82**, 239.
SILCOCK, J. M., HEAL, T. J. & HARDY, H. K. (1955–56). *J. Inst. Met.* **84**, (1), 23.
SOUTHWELL, R. V. (1949). *An Introduction to the Theory of Elasticity*. Oxford: University Press.
THOMAS, G. & WHELAN, M. J. (1959). *Phil. Mag.* **4**, 511.
THOMAS, G. & NUTTING, J. (1959). *Acta Met.* **7**, 515.